eSim 2018
«BUILDING SIMULATION TO SUPPORT BUILDING SUSTAINABILITY»
IBPSA Canada
The Canadian Chapter of the International Building Performance Simulation Association
Le chapitre canadien de International Building Performance Simulation Association

Snow/ground reflectivity model for simulating energy use in buildings

Luminita Dumitrascu[1], Ian Beausoleil-Morrison[1]
[1] Carleton University, Ottawa, Canada

Abstract: *The paper describes the development of an empirical model for predicting ground and snow reflectivity. Ground reflected solar radiation is among the factors having a significant impact on heating/cooling load calculation, solar collector performance, and building energy use prediction. The presence of snow can increase the reflectivity of the ground, leading to increased solar radiation incident on various surfaces of a building. It is common for building performance simulation users to employ the default values of ground reflectivity which can lead to significant inaccuracies, especially for the period when ground is covered by snow. A new model is derived based on point measurements of incoming (global horizontal) and reflected solar radiation taken for a fifteen-month period (December 2016 – March 2018), at Carleton University, Ottawa. An algorithm is developed for three periods: ground free of snow, non-melting or snow accumulation, and melting. The main predictors of reflectivity were found to be the following: zenith angle, cloud cover, and snow age.*

Keywords: *building performance simulation, ground/snow reflectivity, zenith angle, cloud cover, snow age*

INTRODUCTION

Nowadays, architects and engineers are employing more extensively building energy simulation tools for code compliance or for designing more energy-efficient buildings. To decrease the gap between the predicted and actual energy use of a building accurate input information is needed. Weather data, as well as data about the microclimate around the building represent an important component of such input. Ground reflected solar radiation is among the factors having a significant impact on predicting the total solar radiation incident on various surfaces of a building. Accurate modelling of solar radiation incident on a building façade is very important in obtaining reliable predictions regarding the energy use of the building and its thermal performance.

The presence of snow can significantly increase the reflectivity of the ground, leading this way to increased solar radiation incident on various surfaces of the house, particularly the vertical ones (walls and windows). For northerly latitudes, snow covers the ground for more than five months during the winter, creating conditions where ground-reflected solar radiation can be an important fraction of the total radiation incident on surfaces of different orientation. Under such conditions, accurate estimation of the snow reflectivity is required in order to make reliable predictions regarding the performance of a solar technology (Hunt & Calafell, 1977), as well as the performance of the whole building.

Direct surface measurements of snow reflectivity are rarely available, and might contain large errors if the instrumentation is not properly monitored and maintained (Gardner & Sharp, 2010). Empirical models of snow reflectivity can be incorporated in building performance simulation tools, improving this way the reliability of predictions regarding energy use or heating/cooling load calculation, as well as the performance of solar collectors.

According to Natural Resources Canada report on energy efficiency trends between 1990-2013, 83% of all residential energy use was for space and water heating (Natural Resource Canada, 2016). Population growth, along with increased demand for new houses (with bigger square footage, number of appliances, and cooling requirements) is leading to an increase in overall residential energy use (Natural Resources Canada, 2011). For Canadian climate, decreasing the heating load and the energy demand for domestic hot water (DHW) can have a significant contribution to energy use reduction and could lead to a decrease of the greenhouse gases production. Modest levels of passive solar design, as site selection and building orientation, also called sun-tempering, can reduce building auxiliary heating requirements from 5% to 25%. Passive solar houses incorporating more advance features as proper orientation of windows and window-to-wall ratio optimisation, as well as thermal mass can reduce heating energy use by 25% to 75% compared to a typical structure while remaining cost-effective on a life-cycle basis (US Department of Energy, 2016).

Currently, in the building performance simulation field, there are two models used for predicting reflectivity, both for the period when ground is covered by snow: a “simple” and a “complex” one, developed by Thevenard and Haddad in 2006 (see Table 1). The simple model predicts the reflectivity based on the number of days with snow in a month, while the complex one based on the rate of snow

Proceedings of eSim 2018, the 10th conference of IBPSA-Canada
Montréal, QC, Canada, May 9-10, 2018
443
ISBN 978-2-921145-88-6

decay and ambient temperature. Both models require climatic information such as the average number of days with snow depth greater than 5 cm in a month, and the actual daily or hourly snow depth, respectively. The algorithms were tested by simulating a passive solar house, for seven locations in Canada. The advanced and simple model predicted about the same reduction in the sensible heating load. According to the study, the sensible heating load of a passive solar house located in a rural setting can be reduced from 3.2 to 10.1% on a yearly basis, and can reach values as high as 23% on a monthly basis (Thevenard & Haddad, 2006).

Typically, the information regarding snow falls and/or snow depth is either missing from the weather files used for simulation or is not easy to find/very accurate. The new model attempts to predict snow reflectivity employing climatic information existing in the weather files, such as: dry and wet bulb temperature, atmospheric pressure, relative humidity, and global horizontal solar radiation. The steps completed so far, are the following:

- Literature review for identifying the existing models and potential gaps in knowledge;
- Field study for measuring ground/snow reflectivity;
- Analysis of data and derivation of the functional form of the model (the snow melting period currently in work).

The next steps toward the completion of the study are the following:

- Derivation of the functional form for snow melting period;
- Implementation of the model in the ESP-r source code;
- Impact evaluation by comparing the solar radiation received by a vertical and a 60º-tilted surface predicted by the model with measured values.

BACKGROUND

Ground reflectivity or albedo can be defined as the ratio of reflected to incident solar radiation. Reflectivity is used mostly in engineering studies such as simulation of building and solar collectors performance, urban heat island effect, while albedo is specific to astronomy, remote sensing and climatological studies. The terminology albedo and reflectivity are used interchangeably throughout the literature. However, for the purpose of the present paper, only the term surface reflectivity will be used.

Reflectivity depends, in general, on factors such as: the nature of the surface considered, solar elevation/zenith angle, and cloud cover (Nkendirim, 1972), (Arnfield, 1975). For snow covered surfaces, additional factors such as: snow age, accumulated depth, deposition of light absorbing particles (dust and soot), ambient temperature, should also be considered (Muneer, 1997), (Chen, Li, Li, & Liu, 2014).

Studies conducted so far show that ground reflectivity increases significantly in the presence of snow. The values of fresh snow reflectivity reported in literature are between 0.75 (Muneer, 1997) and 0.95 (Backer, Ruschy, & Wall, 1990). In time, snow reflectivity decreases to values between 0.7 and 0.5 or less (Backer, Ruschy, & Wall, 1990).

According to Petzold, snow surface can experience a high day to day variability in reflectivity, which is in sharp contrast to that of a naturally vegetated surface or bare ground (Petzold, 1977). Snow covers the ground for over four months a year in ten of Canada's major cities. The longest periods of lingering snow, with at least a centimetre of snow cover, are found in the following cities: Saguenay, QC-155 days; Sudbury, ON-136 days, Edmonton, AB-133 days, Winnipeg, MB-128 days, and Regina, SK-125 days (Environment Canada, 2017).

In this context, the exact knowledge of snow reflectivity is very important for various applications, such as: heating load calculation, energy use estimation, solar collector efficiency or snow melt prediction.

Specular reflection which is the result of a defined beam reflected off a smooth surface has also influence on snow reflectivity. According to Duffie and Beckman, for most ordinary surfaces, as bare soil and plant covered soil, ground reflectivity is almost entirely diffuse (Duffie & Beckman, 2013). Specularity can increase the reflected radiation either forward or backward. Dirmhirn and Eaton found that the reflectivity of fresh fallen snow is almost isotropic, while the specular component increases with the age of snow (Dirmhirn & Eaton, 1975). A model accounting for specularity was developed by Gueymard, in 1987. However, the ground reflected radiation calculated with his model is very close to the value provided by the isotropic case (Gueymard, 1987). Thevenard and Haddad consider that the additional computational expense to account for specularity does not seem justified in the case of building performance simulation (Thevenard & Haddad, 2006).

SOME GROUND/SNOW REFLECTIVITY MODELS FOUND IN LITERATURE

Starting in early 1960s, ground/snow reflectivity models were developed under a wide range of snow and atmospheric conditions, for various purposes. Depending on their application (earth's heat balance, climatological models, urban heat island effect, performance of solar collectors, building energy simulation) the model development requires input parameters such as: solar zenith angle, snow depth, snow age/rate of decay, concentration of light-absorbing particles, cloud cover index, and temperature (Gardner & Sharp, 2010). Table 1 presents the functional form and the inputs required by some of the most relevant models found in literature.

ISBN 978-2-921145-88-6

Table 1. Relevant snow/ground reflectivity models found in literature

Reflectivity Model	Input Data	Reference
The simple model		
$\rho_{g,i} = \rho_{nosnow} + \left(1 - \frac{N_{snow,i}}{N_i}\right) + \rho_{snow} \cdot \frac{N_{snow,i}}{N_i}$ where: ρ_{nosnow} – snow-free reflectivity of ground ρ_{snow} – snow reflectivity $N_{snow,i}$ – average number of day with snow in month i N_i – number of days in month i	• ρ_{nosnow} – snow-free reflectivity of ground • ρ_{snow} – snow reflectivity • $N_{snow,i}$ – average number of day with snow in month i • N_i – number of days in month i	Thevenard and Haddad (2006) following Liu and Jordan (1963)
The advanced model		
• Assumes real historical record of snow depth is available; • If snow depth increases from the previous time step, reflectivity is set to a high value; • Reflectivity is then reduced with each passing day; • Snow melt is determined applying a simple energy balance at the surface of snow. When snow is less than 5 cm, the following formula is applied: $\rho_g = \rho_{g,nosnow} + \left(1 - \frac{d}{d_0}\right) + \rho_{snow} \cdot \frac{d}{d_0}$ where: d – snow depth d_0 – snow depth 5 cm ρ_{snow} – reflectivity calculated for snow depth greater than 5 cm $\rho_{g,nosnow}$ – month dependent reflectivity	• d – snow depth • d_0 – snow depth 5 cm • $\rho_{g,nosnow}$ – month dependent reflectivity • ρ_{snow} – snow reflectivity	Thevenard and Haddad (2006)
Other models for winter		
$\rho = 0.839 - 0.0473 \cdot n^{1/2}$ where: n – number of days after snowfall	• Number of days after snowfall	Baker et al. (1990)
$\rho = \rho_{min} + (\rho(0) - \rho_{min}) \cdot e^{-\frac{n}{K}}$ where: ρ_0 – reflectivity of snowfall day (0.85) ρ_{min} – converged reflectivity value n – number of days after snowfall K – rate of decrease parameter	• Number of days after snowfall	Kondo and Yamazaki (1990)
$\rho = \rho_{t-1} - DR$ where: ρ_{t-1} – reflectivity from preceding day DR – decay rate	• Maximum temperature • Net solar radiation • Snow depth • Starting reflectivity	Gray and Landine (1987)
For melting season: $\rho = 0.90 - 9.21 \times 10^{-4} \cdot T_{acc} - 0.0042 \cdot SR$ where: T_{acc} – accumulated daily maximum temperature index (ºF) SR – solar radiation (mW/cm^2)	• Temperature • Solar radiation	Winther (1993)
Model for vegetated ground		
For vegetated ground: $\rho = \rho_0 \cdot e^{bz}$ where: ρ_0 – statistical estimate coefficient z – zenith angle (degree) b – coefficient describing the rate of reflectivity changing	• Zenith angle • Surface properties	Arnfield (1975)

ISBN 978-2-921145-88-6

THE FIELD STUDY/DATA COLLECTION

To measure the global horizontal and the reflected solar radiation required for ground/snow reflectivity calculation, a fifteen-month (December 2016 – March 2018) field study was conducted at Urbandale Centre for Home Energy Research, Carleton University, Ottawa, ON (45.38°N, 75.69°W). Urbandale Centre is located on the north-east area of Carleton University campus, and the measurements were performed for a fix point, on a relatively flat (assumed horizontal) field on both south and north sides of the Centre.

The sensor used was a Kipp and Zonen CMA6 albedometer which is sensitive to wavelengths of about 0.3 to 3.0 μm. The albedometer comprises two CMP6 sensing elements and dome assemblies in a single housing, with two signal outputs on one signal connector. Each CMP6 element features a 64-junction thermopile sensing element with a highly absorptive and spectrally flat black coating to capture incoming radiation and convert it to an electrical signal. They are protected by two high-quality concentric domes, 2 mm thick, and the housing is completely sealed. The two high-quality concentric domes reduce directional error and improve thermal isolation. The upper sensor measures incoming global solar radiation and the lower one measures solar radiation reflected from the surface below. When the two signal outputs are converted to irradiance in W/m², the reflectivity can be simply calculated, dividing the reflected radiation to the incoming one (Kip and Zonen, November 2013).

The main sources of error in snow/ground reflectivity calculation are the following: the albedometer, its mounting equipment, and the measurement and recording of the instrument output. Hamilton and Collingbourne have indicated that pyranometers are causing measurement errors due mainly to the dependence of their output on temperature and on the solar azimuth and zenith angles, as well as due to their inherent non-linearity (Hamilton & Collingbourne, 1967). According to Kipp and Zonen, when performing reflectivity measurements with a CMA6 albedometer, the non-stability error is smaller than 1%, the non-linearity error is also smaller than 1%, the temperature error is smaller than 4%, while the tilt response error is smaller than 1% (Kip and Zonen, November 2013). The estimated instrument calibration uncertainty was calculated to be ± 2.57%. The albedometer was mounted horizontally, and it was kept at 1.5 m height above the snow/ground surface, to promote spatial averaging. Efforts were made to minimize shading at low solar elevation by rotation of the instrument. According to calculations performed using the method outlined by Slatyer and Mcllroy (Slatyer & Mcllroy, 1961) the shaded area due to the mounting equipment was less than 0.15% and as such, no adjustment in reflectivity values was made to correct the influence of the shaded area. Accurate measurement of the global radiation requires proper levelling of the detector surface. Efforts were made to level the instrument properly, by bringing the bubble of the spirit level centrally within the marked ring.

The incident and reflected radiation were measured every second. For the period December 2016 – July 2017, the 1 second time interval measurements were averaged and store every 5 seconds by a National Instruments cFP 2220 data logger. The relative offset error of the National Instruments cFP 2220 data logger was ± 6.23%, and it adds to the albedometer uncertainty. The root-sum-square error analysis was applied to find the total bias error associated with reflectivity calculation. For the period December 2016 – July 2017, the total bias error was found to be ± 8.4%. For the period August 2017 – March 2018, a National Instruments PXIe 1078 data logger is used, the relative offset error being in this case only ± 0.04%. The total bias error associated with reflectivity calculation was found to be ± 5.7%. In addition to measurements of global horizontal and reflected solar radiation, daily observations of snow fall events, snow properties/conditions, depth and age, cloudiness were made daily. Similar observations were made also for the period when the ground is free of snow.

DATA ANALYSIS AND OBSERVATIONS

According to the albedometer mounting instructions, the device should be located at a distance at least ten times bigger than the highest obstacle, such as no shadow will be casted upon device at any time. However, the site available for performing the measurements did not meet the above requirement, and for sunny days, at low solar altitude, some of the surrounding trees were casting shadows on the device and the surface below for approximately one hour after sunrise and half an hour before sundown. Moreover, for cold days, due to the high difference between the ambient temperature and the device temperature (for security reasons, the device was kept inside Urbandale Centre overnight), at least 10-20 minutes were required for the instrument to stabilize. The measurements corresponding to those time intervals were eliminated from analysis, to avoid uncharacteristic values of the reflectivity.

The initial data analysis was performed for the period December 2016 – April 2017 (only the days when ground was covered by snow). However, the resulting functional form of the model failed to capture the rapid decay of the reflectivity due to the accelerate snow melt towards the end of the period. In order to improve the accuracy of the model it was decided to divide the data into two periods:

- Non-melting or accumulation period – snow decay very small, frequent snow falls, and ambient temperature mostly below 0°C;
- Melting period – snow decay very rapid, isolated snow falls, and ambient temperature frequently above 0°C.

For both seasons, ground free of snow and ground covered by snow, average daily reflectivity was calculated and

ISBN 978-2-921145-88-6

plotted versus time to observe the annual, monthly, and daily trend. Figure 1 illustrates the seasonal variation of daily average reflectivity.

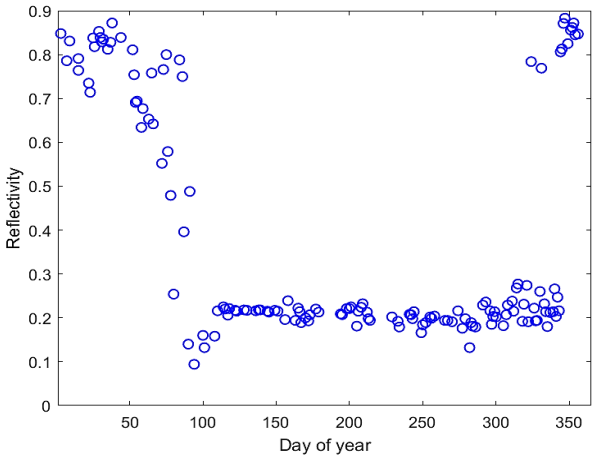

Figure 1. Seasonal variation of average daily reflectivity

As Figure 1 shows, during the accumulation period, snow reflectivity has a small variation around the average value of 0.8. By contrast, the melting period was characterized by high rates of reflectivity decay, the average daily reflectivity being 0.580. Significant or complete melting of snow cover was also noticed in some days. In general, the transition from the accumulation to the melting period is signalled by a sharp change in reflectivity trend (observed near day 50).

The duration of accumulation and melting period is highly dependent on the site location and the weather conditions at that site. Multiple criteria, such as snow cover melting, reflectivity decay rate, and ambient temperature should be considered when deciding the beginning of the melting period.

Sky transmissivity is defined as the ratio between the global radiation incident on a horizontal surface and the extra-terrestrial radiation incident on a horizontal plane. Variation of the earth-sun distance lead to variations of the extraterrestrial radiation flux in the range ±3%. For engineering calculations, extraterrestrial radiation incident on the plane normal to the radiation on the n^{th} day of the year (G_{on}), in W/m^2, is calculated using the formula (Carroll, 1985):

$$G_{0n} = G_{sc}\left[1 + 0.033 \cdot cos\left(\frac{360 \cdot n}{365}\right)\right] \qquad (1)$$

where G_{sc} is the solar constant (1367 W/m^2) and n is the day of year.

Extraterrestrial radiation incident on the surface tangent to the outer surface of the atmosphere (G_o), in W/m^2, is given by the formula (Carroll, 1985):

$$G_0 = G_{0n} \cdot \cos(\theta_z) \qquad (2)$$

where G_{0n} is the extraterrestrial radiation incident on the plane normal to the radiation [W/m^2] and $\theta_z$is the zenith angle [degrees].

The total solar radiation or global radiation incident on a horizontal surface was measured at 5 second time interval and averaged minutely. The zenith angle was also calculated minutely, using the values of solar altitude provided at one-minute time step by the United States Naval Observatory (USNO), Sun or Moon Altitude/Azimuth Calculator (USNO, 2017). The extraterrestrial solar radiation incident on a horizontal surface was calculated using equations (1) and (2). Finally, the sky transmissivity for every minute (ST) was found as the ratio between the measured global radiation incident on a horizontal surface and the calculated extraterrestrial solar radiation on a horizontal surface. Sky transmissivity was used as an indicative of cloudiness. Analysing the values of global horizontal radiation, sky transmissivity, and the daily records regarding the sky cloud cover, it was noticed that sky transmissivity has values less than 0.3 for overcast sky, between 0.3 and 0.6 for intermittent cloudiness or mixed sky, and higher than 0.6 for clear sky. Figure 2 illustrates the daily variation of reflectivity with the zenith angle for three representative types of cloud cover: clear sky, mixed sky or intermittent cloudiness, and overcast sky.

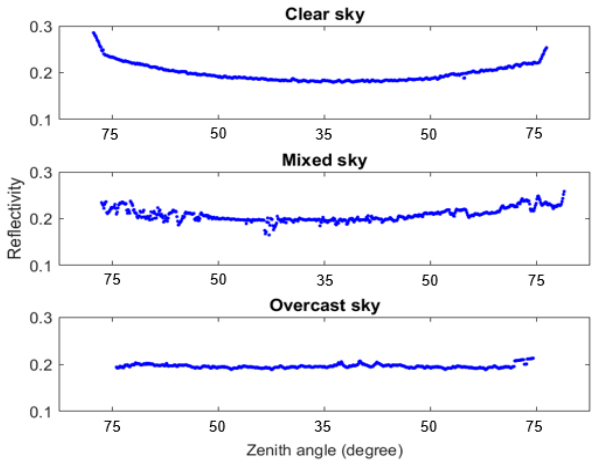

Figure 2: Daily variation of reflectivity with zenith angle and cloud cover

For both seasons, ground covered by snow and ground free of snow, there is a positive correlation between reflectivity and the solar zenith angle (reflectivity increases with the increase of the zenith angle). A positive correlation was also noticed between reflectivity and sky transmissivity (for equal zenith angles, the reflectivity is higher when the sky transmissivity is higher). During the winter season, the variation was noticed to be around the mean value of 0.8, while for the free of snow period the variation was around the mean value of 0.2.

ISBN 978-2-921145-88-6

Some of the observations made during the data analysis process may be summarized as follows:

- The observed snow reflectivity displays a small variance during the winter months (monthly average 0.004). The variance increases 10-fold during the snow melting season (monthly average 0.038).
- During the snow accumulation period, the reflectivity is rarely below 0.75 and very often the values exceed 0.85 due to new snowfall events.
- According to literature, reflectivity depends on numerous factors such as: particle size, wetness, and impurities accumulation. Visual observation of the snow cover led to the conclusion that fresh dry/powdery looking snow (very frequent during accumulation period) might have average reflectivity as high as 0.9, while fresh snow with a high content of water (frequent during snow melting period) around 0.8 or lower. Likewise, clean snow, one-week old might have average reflectivity around 0.7, while one week old snow with a high level of particulate matter accumulation (dust and soot) as low as 0.45.
- At the end of the active melting of snow, the reflectivity has the average value of 0.17 and it can reach values as low as 0.07 (typical value for water), depending upon the presence of a continuous film of water at the ground surface.
- The variation of snow reflectivity increases with the zenith angle. As Figure 2 illustrates, the variation of reflectivity with the zenith angle is more noticeable on clear sky days than on days with overcast sky. According to literature (Nkendirim, 1972), the lower values of reflectivity noticed on overcast days is a consequence of the sky being the effective radiator instead of the sun.
- For similar zenith angles, the values of reflectivity before noon are slightly higher than the afternoon ones. According to literature, the difference in spectral composition of light from morning to afternoon, as well as the state of vegetation (weltering in the afternoon) or snow surface (more particulate matter accumulation) may account for this phenomenon.
- The reflectivity decreases with snow age. The average daily decreasing rate of reflectivity due to snow age was found to be 2.2% for the snow accumulation period and 17.1% for the snow melting period.

MODEL FORMULATION

The study was focused on investigating the relationships between reflectivity and zenith angle, snow age and cloud cover, respectively. All snow reflectivity models referenced in literature have as predictors only one or two of the above-mentioned variables. The present model was developed assuming that all the above-mentioned parameters have significant influence on snow reflectivity, and as such all three were considered to be predictors for the model. In order to test the assumed hypothesis, the p-value method was applied. The hypothesis test was conducted for a 99% confidence interval and the corresponding p-values led to the conclusion that all variables are significant.

The snow/ground reflectivity was calculated from measurements of incoming and reflected solar radiation, recorded at 5 second time interval, and averaged minutely. The zenith angle (in degrees) and the sky transmissivity (unitless) were also calculated every minute. The snow age (in hours) was calculated based on the observations made at the site during the data collection period. The analyses of reflectivity for the period from December 2016 to December 2017, and the observations made during the data collection period, led to the conclusion that significant changes of both daily and long-term reflectivity can be associated with the following periods:

Short grass covered ground

Represents the period starting with the second half of April, until the first half of November, when the ground is generally completely free of snow. After the melting of snow, for a few days, the ground reflectivity varies slightly around the average value of 0.17 (ground saturated with water). While the water concentration at the ground surface decreases, and the grass starts growing, the reflectivity registers small variation around the average value of 0.2, cited in literature as characteristic for short grass (Thevenard & Haddad, 2006).

To study the relationship between variables the statistical method of multiple regression was used. The linear relationship provided by the multiple regression procedure was slightly adjusted to better fit the measured data. The functional form which best describes the relationship is the following:

$$\rho = 0.175 + 0.07*[1 - \cos(\theta_z)] + 0.04*ST - 0.0009*(50 - \theta_z) \quad (3)$$

where ρ is reflectivity [decimal], θ_z is the zenith angle [degrees] and ST is sky transmissivity [decimal].

The statistical analysis performed on this set of data shows that the adjusted R-squared is 0.68. The analysis of residuals (the difference between the observed and predicted value) shows that the mean absolute error (MAE) is 0.011, standard deviation 0.0146, and sample variance 0.0002. Even though the value of adjusted R-squared indicates a moderate correlation, as Figure 3, presenting the plot of observed and predicted reflectivity versus zenith angle exemplifies, there is a good fit between the trends of measured and predicted data for most days. Furthermore, the MAE has a value significantly lower than the measurement error, indicating that the predicted values are in close agreement with the observed ones.

ISBN 978-2-921145-88-6

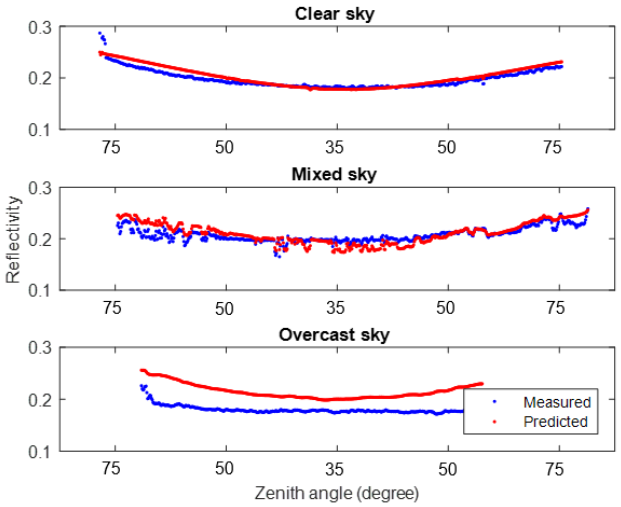

Figure 3. Observed and predicted reflectivity versus zenith angle for representative days (no snow)

The sample of observed data was manually sorted in three bins: days with clear sky (most of the time sky transmissivity higher than 0.6), days with mixed sky or intermittent cloudiness (sky transmissivity between 0.3 – 0.6), and days with overcast sky (sky transmissivity lower than 0.3 most of the time). As Figure 3 illustrates, for clear and mixed sky, the model is slightly overpredicting the reflectivity at the beginning and at the end of the day. For days with overcast sky, when sky transmissivity has very low values (many times lower than 0.1), the values predicted by the model display a higher difference compared with the measured ones. Taking into account that for these time intervals the solar radiation has very low values, the error introduced in calculation of the solar radiation incident on surfaces of various orientations might be insignificant. After the implementation of the model in the ESP-r source code, and the quantification of the error between the measured and predicted incoming solar radiation, the algorithm can be adjusted to account for this difference, decreasing this way the error between the measured and predicted values.

Accumulation or non-melting period

Represents generally the period starting at the end of November/beginning of December, until the beginning of active melting of snow. As previously was said, during this period there are frequent snow fall events and the decrease of reflectivity between them is relatively small.

In order to assess the influence of snow age on reflectivity, the difference between the average reflectivity of a day with fresh snow and the average reflectivity of the last day before a new snow fall event was calculated. The decreasing rate of reflectivity was calculated as the ratio between this difference and the number of days between two consecutive snow events. The decreasing rate was noticed to be in the range of 0.4% to 3.8% per day, with an average of 2.2% per day.

Similar with the case of ground free of snow, the statistical method of multiple regression was used to study the relationship between variables. A new variable, snow age (SA) was added for the snow accumulation season.

In addition to measurement of global horizontal and reflected solar radiation, a daily "weather log" was kept in order to record information such as: snow fall events (duration, qualitative observation as heavy, moderate or light), snow properties/conditions (fine/large flakes, dry/wet), snow depth and age, as well as cloudiness (qualitative observation clear sky, mixed or overcast). Every morning, before starting the measurement of reflected and global horizontal solar radiation, the snow depth was measured and the snow age, in hours, was set to a value equal to the number of hours since the last snow fall.The value was increased minutely until the occurrence of a new snow fall event.

During the accumulation period, it was noticed that snow age does not have a significant impact on diurnal variation of reflectivity. The effect of snow decay was more noticeable when comparing the reflectivity at the beginning of a day with the one corresponding to the beginning of previous day.

The linear relationship provided by the multiple regression procedure was also slightly adjusted to better fit the measured data. The functional form which best describes the relationship is the following:

$$\rho = 0.9 - 0.03*[1-\cos(\theta_z)] - 0.1*ST \\ -0.015*(SA/24) \quad (4)$$

where ρ is reflectivity [decimal], θ_z is the zenith angle [degrees], ST is sky transmissivity [decimal] and SA is the snow age [hours].

As in the previous case, a statistical analysis was performed, and the adjusted R-squared value was found to be 0.64. The analysis of residuals (the difference between the observed and predicted value) shows that the mean absolute error (MAE) is 0.037, standard deviation 0.049, and sample variance 0.002.

Similar with the ground free of snow period, the value of adjusted R-squared indicates a moderate correlation between variables. However, the adjusted R-squared is a relative measure of fit and when the goal is to use the model for prediction, its value is not very relevant (Agami Reddy, 2011). As Figure 4, presenting the plot of observed and predicted reflectivity versus zenith angle illustrates, there is a good fit between the trends of measured and predicted data for most days. Furthermore, the MAE has a value significantly lower than the measurement error, indicating that the predicted values are in close agreement with the measured ones.

ISBN 978-2-921145-88-6

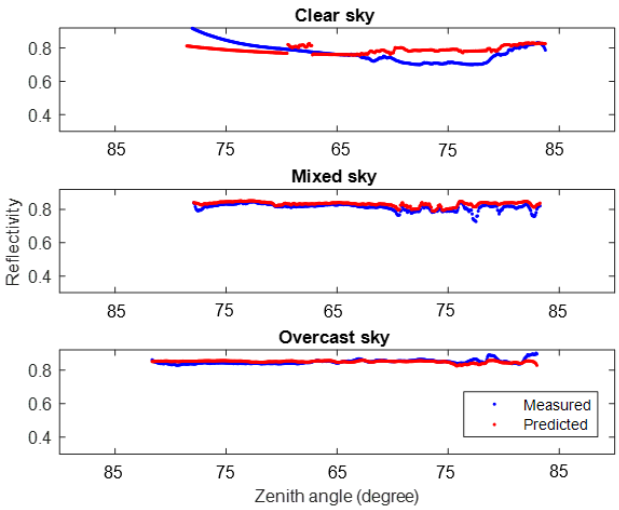

Figure 4. Observed and predicted reflectivity versus zenith angle for representative days (snow accumulation)

From Figure 4 it can be noticed also that for days with mixed and overcast sky, the values predicted by the model follow the trend of observed data very closely most of the time. However, in the case of days with clear sky, there are noticeable differences between the trends of observed and predicted data, especially for high transmissivity and high zenith angles. This can be partly explained by the small number of sunny days during the accumulation period, when the days with mixed and overcast sky are dominant. Taking into account that for these time intervals the solar radiation has low values, the error introduced in calculation of the solar radiation incident on surfaces of various orientations might not be significant. After the implementation of the model in the ESP-r source code, and the quantification of the error between the measured and predicted incoming solar radiation, as in the case of ground free of snow, the algorithm can be adjusted to account for this difference, decreasing this way the error between the measured and predicted values.

Melting period

Represents the period from the beginning of active melting of snow until the ground is completely free of snow. The start of melting period is established generally based on the observation of snow fall events and the values of ambient temperature (no snow falls and positive value for a few consecutive days). During this period, the snow fall events are less frequent and reflectivity decreases significantly between them. The decreasing rates of reflectivity were noticed to be in the range of 0.9% to 47.1% per day, with an average of 17.1% per day. It was also noticed that the values of snow reflectivity span over a wide range (0.25 – 0.95), being in sharp contrast with the snow accumulation period, when reflectivity has small variations around the 0.8 value.

Due to the very low temperatures registered in February and March 2018, the data collection for the melting period was extended until the end of March/beginning of April. The analysis of the data is still in progress, and as such no functional form is available at the moment for this period.

NEXT STEPS

Currently, the analysis for deriving the functional form of the melting period is under way. Based on the work completed so far it was noticed that the sharp irregularities of the melting period are hard to capture in a single continuous function. A piecewise function, dividing the day in two periods: temperature below and above 0°C might be an option for improving the performance of the model.

After completing the development of the functional form, the model will be implemented in the ESP-r source code. The inputs required by the model are the solar zenith angle and sky transmissivity for the period when ground is free of snow and the solar zenith angle, sky transmissivity and snow age for the period when snow covers the ground. The solar module of ESP-r has the capability of calculating the solar zenith angle. Employing the values of the zenith angle provided by the solar module, and the equations (1) and (2) presented in this paper, the algorithm will calculate the sky transmissivity for each time step. Further, using the functional form characteristic for the ground free of snow period, the reflectivity will be calculated for each time step of the simulation process.

In order to switch from the period when the ground is free of snow to the period when it is covered by snow, it is necessary to use some criteria or flags. The presence of snow, predicted by the algorithm based on the dry and wet bulb temperature, atmospheric pressure and relative humidity will be used as first flag. When snow is detected the algorithm will start counting the snow age for every time step. If the presence of snow is detected for a specific number of hours (the number of hours will be established based on a trial and error procedure, comparing the predicted reflectivity with the measured one) the algorithm switches from the summer model to the accumulation one. Based on the calculated values of zenith angle, sky transmissivity and snow age, the reflectivity will be predicted for each time step of the simulation.

A second flag will be used to choose between the model for the accumulation and melting period. Based on the observations made during the data collection period, it was noticed that snow reflectivity decreases significantly when the outdoor temperature registers values above 0°C and the incoming solar radiation has values at least between 300-500 W/m^2. The algorithm will change from the accumulation to the melting period whenever the temperature and the incoming solar radiation are higher than the established threshold values. When the reflectivity

ISBN 978-2-921145-88-6

reaches the value 0.2 the algorithm will switch again to the ground free of snow model.

In order to assess the performance of the model, a real weather file will be used and the values of reflectivity provided by the simulation will be compared with the measured ones. Further, the model will be used to find the total solar radiation incident on a vertical surface and on a 60°-tilted surface. The simulated values will be compared with measured values. Depending on the accuracy of the results, the modal might be subject to small changes, for improving its performance.

CONCLUSIONS

Accurate predictions of the energy use of a building or the performance of a solar collector require appropriate values of snow/ground reflectivity. Usually, ground reflectivity has no significant variation from one day to another. However, in the case of ground covered by snow, the reflectivity increases significantly, depending on the environment, and it might register important daily and long term variations, as Figure 1 illustrates. In Canada, depending on the region, snow covers the ground up to six months per year. For these months, the solar radiation reflected by the snow becomes a significant component of the total solar radiation incident on various facades of a building. Many times, the energy use picks also during the winter season. Taking into account the increased fraction of solar radiation while designing new buildings or retrofitting existing ones may offset a significant part of the energy use associated with the built environment. For example, the mean reflectivity of ground covered by short grass was found to be 0.208±0.057, while the mean reflectivity for snow was 0.843±0.057 for the accumulation season and 0.587±0.057 for the melting season, respectively.

Direct surface measurements of snow reflectivity are rarely available, and they might contain large errors due to improper maintenance and monitorization of the instruments. Empirical models of ground/snow reflectivity can be incorporated in building performance simulation tools, improving this way the reliability of predictions regarding energy use or heating/cooling load calculation, as well as the performance of solar collectors.

A relationship between the snow reflectivity and the zenith angle, sky transmissivity and snow age was developed for three periods:

- Ground free of snow;
- Non-melting or accumulation period – snow decay very small, and frequent snow falls;
- Melting period – snow decay very rapid, and isolated snow falls.

For the ground free of snow model the input data are the zenith angle and sky transmissivity, while for the ground covered by snow period a third input variable, snow age is added. Even though the correlation coefficients are not very close to the ideal value of 1, as the visuals presented throughout the paper show, most of the time there is a good agreement between the measured and predicted trends. The study is still under way, and more data will be collected for the winter season for further improvement of the model. Using an independent set of data, the model will be also empirically validated, by comparing the predicted values with the measured ones. Additional work will be performed to implement the model in the ESP-r source code to quantify the effect of the snow/ground reflectivity models on prediction of solar radiation incident on surfaces of different orientation. The solar irradiance incident on a south oriented vertical surface and on a 60º-tilted surface will be simulated using the model. The values provided by the simulation will be compared with measured data.

REFERENCES

Agami Reddy, T. (2011) *Applied data analysis and modeling for energy engineers and scientists.* New York. Springer.

Arnfield, A. (1975). A note on the diurnal, latitudinal and seasonal variation of the surface reflection coefficient. *Journal of Applied Meteorology, 14*, 1603-1607.

Backer, D., Ruschy, D., and Wall, D. (1990). The albedo decay of prairie snows. *Journal of Applied Meteorology*, (29), 179-187.

Carroll, J. J. (1985). Global transmissivity and diffuse fraction of solar radiation for clear and cloudy skies as measured and as predicted by bulk transmissivity models. *Solar Energy*, *35*(2), 105-118.

Chen, A., Li, W., Li, W., and Liu, X. (2014). An observational study of snow aging and the seasonal variation of snow albedo by using data from Col de Porte, France. *Chinese Science Bulletin*, *59*(34), 4881-4889.

Dirmhirn, I. and Eaton, F. (1975). Some characteristics of the albedo of snow. *Journal of Applied Meteorology, 14*, 375-379.

Duffie, J. and Beckman, W. (2013). *Solar Engineering of Thermal Processes.* Hoboken, New Jersey: John Wiley & Sons, Inc.

Gardner, A. and Sharp, M. (2010). A review of snow and ice albedo and the development of a new physically based broadband albedo parametrization. *Journal of Geophysical Research, 115*.

Graham, W. and King, K. (1961). Shortwave reflection coefficient for a field of maize. *Journal of Applied Meteorology,* (2), 425-428.

Gray, D. M. and Landine, P. G. (1987). Albedo model for shallow prairie snow covers. *Canadian Journal of Earth Science, 24*, 1760-1768.

ISBN 978-2-921145-88-6

Gueymard, C. (1987). An isotropic solar irradiance model for tilted surfaces and its comparison with selected engineering algorithms. *Solar Energy, 38*(5), 367-386.

Hamilton, R. A. and Collingbourne, R. H. (1967). A difficulty in the interpretation of certain radiation measurements. *Quarterly Journal of the Royal Meteorological Society, 93*, 186-194.

Henneman, H. E. and Stefan, H. G. (1999). Albedo models for snow and ice on a freshwater lake. *Cold Regions Science and Technology, 29*, 31-48.

Hunn, B. and Calafell, D. (1975). Determination of average ground reflectivity for solar collectors. *Solar Energy, 19*, 87-89.

Kip and Zonen. (November 2013). Instruction manual: CMP series Pyranometer, CMA series Albedometer.

Kondo, J. and Yamazaki, T. (1990). A predisction model for snowmelt, snow surface temperature and freezing depth using a heat balance method. *Journal of Applied Meteorology, 29*, 375-384.

Liu, B. and Jordan, R. (1963). The long-term average performance of flat-plate solar energy collerctors. *Solar Energy, 7*, 53-74.

Muneer, T. (1997). *Solar Radiation and Daylight Models for the Energy Efficient Design of Buildings.* Oxford: Architectural Press.

Natural Resources Canada. (2011, December). *Energy Efficiency Trends in Canada 1990 to 2009.* Retrieved November 2, 2016, from http://www.oee.nrcan.gc.ca/publications/statistics/trends11/trends.pdf

Natural Resource Canada. (2016). *Energy Efficiency Trends in Canada 1990-2013.* Natural Resources Canada. Retrieved from https://www.nrcan.gc.ca/sites/www.nrcan.gc.ca/files/energy/pdf/trends2013.pdf

Nkendirim, L. (1972). A note on the albedo of surfaces. *Journal of Applied Meteorology*, (11), 867-874.

Petzold, D. E. (1977). An estimation technique for snow surface albedo. *Climatological Bulletin, McGill University, 21*, 1-11.

Slatyer, R. O. and Mcllroy, I. C. (1961). *Practical Microclimatology.* Melbourne: CSIRO.

Stanhill, G., Hofstede, G. and Kalma, J. (1966). Radiation balance of natural and agricultural vegetation. *Quarterly Journal of Royal Meteorology Society*, (92), 128-140.

Thevenard, D. and Haddad, K. (2006). Ground reflectivity in the context of building energy simulation. *Energy and Buildings*, (38), 972-980.

US Department of Energy (2016). *Passive Solar Homes Design.* Retrieved from https://energy.gov/energysaver/energy-efficient-home-design/passive-solar-home-design

ISBN 978-2-921145-88-6